Construction Materials

Environmental impact and durability of carbonated calcium silicate concrete
Jain, Seth and DeCristofaro

ice | proceedings

Proceedings of the Institution of Civil Engineers

http://dx.doi.org/10.1680/jcoma.17.00004
Paper 1700004
Received 20/01/2017 Accepted 26/09/2017
Keywords: concrete technology & manufacture/environment/sustainability

ICE Publishing: All rights reserved

ice Institution of Civil Engineers
publishing

Environmental impact and durability of carbonated calcium silicate concrete

Jitendra A. Jain PhD
Senior Research Scientist, Research and Development, Solidia Technologies Inc., Piscataway, NJ, USA (corresponding author: jjain@solidiatech.com) (Orcid:0000-0002-2423-3533)

Anuj Seth PhD
Technology Director, Research and Development, Solidia Technologies Inc., Piscataway, NJ, USA (Orcid:0000-0002-4651-5558)

Nicholas DeCristofaro PhD
Chief Technology Officer, Solidia Technologies Inc., Piscataway, NJ, USA

This paper describes the environment impact of low-lime calcium silicate cement (CSC) that cures by a reaction with gaseous carbon dioxide. The production of CSC requires less limestone and lower kiln temperatures than those used for ordinary Portland cement (OPC). This makes it possible to reduce the carbon dioxide emissions at the cement kiln from ~810 kg/t for OPC to ~565 kg/t for CSC. The carbon dioxide used in the curing process and captured within CSC-based concrete is industrial-grade carbon dioxide sourced from waste flue gas streams. The fully hardened CSC concrete will contain up to 300 kg of carbon dioxide per tonne of cement used in the concrete formulation. This paper also summarises the performance and durability of CSC concrete (CSC-C) and OPC concrete (OPC-C). Freeze–thaw and scaling resistance were evaluated as per ASTM C666 and ASTM C672, respectively, the concentrations of ionic species leached from the concretes were measured, efflorescence was evaluated in pavers partially submerged in water, and the expansion and mass changes associated with the exposure to sodium sulfate and magnesium solutions were measured. In each of the durability tests, the CSC-C specimens, made with commercially produced Solidia Cement™, performed equivalently or better than the OPC-C specimens.

1. Introduction

Concrete is the most consumed man-made material in the world (UNEP, 2010). A typical concrete is made by mixing ordinary Portland cement (OPC), water and aggregate (sand and crushed stone). OPC is a synthetic material made by burning a mixture of ground limestone and clay, or materials of similar composition, in a rotary kiln at a sintering temperature of 1450°C (WBCSD, 2009). OPC manufacturing releases considerable quantities of carbon dioxide. The cement industry accounts for ~5% of global anthropogenic carbon dioxide emissions (Boden *et al.*, 2014; IPCC, 2007).

A modern cement plant releases ~810 kg of carbon dioxide per tonne of cement clinker produced (DeCristofaro, 2016a). More than 60% of this carbon dioxide comes from the chemical decomposition, or calcination, of limestone as shown in Reaction I.

I. $CaCO_3 \rightarrow CaO + CO_2$

The balance comes from the combustion of fossil fuel to heat the kiln. A small amount of additional carbon dioxide, ~90 kg/t of cement, is associated with the electricity required to grind and transport materials throughout the process, and is not considered in this paper (DeCristofaro, 2016a).

The International Energy Agency (IEA) has created a roadmap to guide the long-term sustainability efforts of the cement industry. As per this roadmap, the cement industry must reduce its total carbon dioxide emissions from 2·0 Gt in 2007 to 1·55 Gt by 2050 (Barcelo *et al.*, 2014). However, over this same period, cement production is projected to grow from 2·6 Gt to 4·4 Gt (Barcelo *et al.*, 2014; WBCSD, 2009).

With the implementation of energy-efficient production technologies, the use of alternative fuels, the development of new, low-lime cement chemistries and the reduction of clinker factors in cement through the addition of supplementary cementitious materials, the cement industry has tried to attain the IEA objective. However, even the combined effect of these initiatives is likely to fall far short of the IEA goals.

Solidia Cement, a revolutionary, new product developed by Solidia Technologies, is poised to address this unanswered challenge (Riman and Atakan, 2012; Riman *et al.*, 2013). Solidia Cement is a reduced-lime, non-hydraulic calcium silicate cement (CSC) that is capable of significantly reducing energy requirements and carbon dioxide emissions at cement plants. The Solidia Cement making process is adaptable and flexible, allowing it to be produced under a variety of raw materials formulations and production methods across the globe. It offers cement manufacturers considerable savings in

Offprint provided courtesy of www.icevirtuallibrary.com
Author copy for personal use, not for distribution

carbon dioxide emissions, energy consumption and costs. Additionally, this CSC cures via a reaction with gaseous carbon dioxide, thus offering the ability to permanently and safely sequester carbon dioxide.

2. Energy requirements and carbon dioxide emissions during cement manufacturing

Both OPC and CSC manufacturing require significant amounts of energy and emit significant quantities of carbon dioxide. Heat energy is needed to dry the raw meal, calcine the limestone, react the oxide components and form the cement clinker. Electrical energy is needed to crush and grind the raw materials, to comminute the clinker and to transport materials throughout the process. To illustrate the benefits associated with the processing of CSC, the differences in energy consumption and carbon dioxide emissions are discussed below.

2.1 OPC

2.1.1 Energy requirements for OPC

In modern cement plants, the production of 1 t of OPC clinker requires heat energy totalling 3·2 GJ and electrical energy totalling 0·4 GJ (Madlool *et al.*, 2011). From a theoretical perspective, the thermal energy consumed in producing 1 t of OPC clinker is about 1·824 GJ (WBCSD, 2009). The breakdown of that enthalpy into the various pyro-processing steps is provided in Table 1 (Taylor, 1997). While the overall process is endothermic, the process step in which the cement phases are formed is exothermic. The difference between the actual and theoretical heat requirements is due to heat retained in the clinker, heat losses from the kiln dust and exit gases, and heat losses from radiation. As can be seen from Table 1, the pyro-processing step that consumes the most heat energy is the endothermic decomposition of calcium carbonate (calcination).

2.1.2 Carbon dioxide emissions for OPC

Historical estimates indicate that 900–1100 kg of carbon dioxide is emitted for every tonne of OPC produced in the USA. The exact quantity depends on the raw ingredients, fuel type and the energy efficiency of the cement plant (EPA, 2005). Even the most efficient Portland cement facilities report carbon dioxide emissions of ∼900 kg/t of clinker (Marceau *et al.*, 2006).

There are three sources of carbon dioxide emissions in cement production.

- The chemical decomposition of the calcium carbonate within limestone (Reaction I).
- The combustion of fossil fuel to heat the kiln for pyro-processing the raw meal.
- The generation of electricity needed to drive the grinding mills and materials transportation systems.

The carbon dioxide emissions from the chemical decomposition of calcium carbonate depend on the lime content of the clinker product, ∼70% for OPC (IPCC, 2007). The carbon dioxide emissions from pyro-processing depend on the fossil fuel type (e.g. ∼3·0 t of carbon dioxide per tonne of coal consumed). The carbon dioxide emissions associated with electricity are about 90 kg/t of cement clinker; these are ignored in this analysis. Table 2 compares the first two sources of carbon dioxide emissions in the production of cement clinkers.

2.2 CSC

2.2.1 Energy requirements for CSC

The total lime content of CSC clinker is in the range of 45–50 wt%, representing ∼30% reduction from that required for OPC. This reduction in lime concentration translates directly into a 30% reduction in the major component of the theoretical enthalpy, that is, the calcination step. CSC and OPC are roughly equivalent in terms of the enthalpy required to decompose the clay component of the raw meal and the exothermic reaction associated with the formation of the cement phases. Dominated by the large difference in the calcination step, the total enthalpy of formation of CSC clinker is expected to be about 1·051 GJ, almost 40% lower than that of OPC clinker (see Table 1).

Table 1. Theoretical enthalpy of formation of 1 t of clinker

Reaction	OPC clinker ΔH: GJ	CSC clinker ΔH: GJ
Calcination	+2·138	+1·514
Decomposition of clay	+0·063	+0·075
Formation of cement phases	–0·377	–0·538
Total	1·824	1·051

OPC clinker values are from Taylor (1997); CSC clinker values are based on a modelled clinker and may vary slightly depending on the phase composition

Table 2. Carbon dioxide emissions during the production of OPC and CSC clinker

Carbon dioxide emissions from	Per tonne of OPC clinker: kg	Per tonne of CSC clinker: kg
Limestone decomposition	540	375
Fossil fuel combustion	270	190
Total carbon dioxide emissions	810	565

Note: The carbon dioxide associated with electrical energy usage in the cement-making process is not considered

Offprint provided courtesy of www.icevirtuallibrary.com
Author copy for personal use, not for distribution

From a practical perspective, CSC clinker is burned at temperatures ~250°C lower than those used in OPC manufacturing, and with the potential for significantly reduced system-wide heat losses than those experienced in OPC manufacturing. This is expected to translate into a reduction in fossil fuel consumption by as much as 30%. The relatively soft Solidia Cement clinker is expected to grind more easily than its Portland cement counterpart. This may translate into additional savings in the electrical energy required for clinker grinding.

2.2.2 Carbon dioxide emissions for CSC

The unique, low-lime content of CSC clinker enables two separate opportunities to reduce the carbon dioxide emissions associated with cement production.

The first opportunity can be traced to the chemical decomposition of the calcium carbonate in limestone. Reduction in the lime content of the cement from 63% (for OPC) to 44% (for CSC) as shown in Table 3 enables a proportionate reduction in this form of carbon dioxide emissions. Thus, the carbon dioxide released from the chemical decomposition of limestone will be reduced from 540 kg/t of OPC clinker to about 375 kg of carbon dioxide per tonne of CSC clinker.

The second opportunity, also enabled by the low-lime chemistry of CSC, allows the reaction between lime and silica to occur at a clinker temperature of 1200°C, which is 250°C lower than the temperature required for OPC clinker formation. During the production of CSC, the carbon dioxide emissions associated with the burning of fossil fuel to heat the kiln are expected to be 190 kg/t of clinker, compared with 270 kg/t for OPC clinker (DeCristofaro and Sahu, 2013).

The total carbon dioxide emissions associated with OPC and CSC manufacturing are compared in Table 2. Note that CSC clinker production offers the potential to reduce carbon dioxide release associated with cement manufacturing by 30%. This value has been confirmed in industrial-scale CSC clinker production (DeCristofaro *et al.*, 2017).

3. Concrete mixing, forming and curing processes

CSC concrete (CSC-C) and OPC concrete (OPC-C) are manufactured using the same basic mixing and forming processes. Concrete production typically begins by mixing dry (cement, sand and crushed stone) and liquid (water and chemical additives) components. The water and chemical additives control the flow behaviour of the concrete mix while it is in the plastic stage.

Both OPC-C and CSC-C can be mixed in standard concrete mixers. Similarly, they can be formed into the final concrete part shape by the same processes and equipment. These processes include casting, extrusion, rolling and pressing.

OPC-C and CSC-C differ in the chemical process by which they set and harden. These processes are collectively referred to as 'curing'.

3.1 OPC-C curing

When OPC is exposed to water, a series of hydration reactions is initiated with the release of a significant amount of heat. These hydration reactions are responsible for the setting and hardening of the OPC-C. In a very simplistic way, the curing process involves reactions including

- C_3A, gypsum and water to produce ettringite
- C_3S and water to produce a complex calcium silicate hydrate and calcium hydroxide
- C_2S and water, which also yields calcium silicate hydrate and calcium hydroxide.

The complex calcium silicate hydrate is an amorphous phase wherein the calcium/silicon ratio can vary during the hydration period.

The hydration of the calcium silicate components of OPC begins as soon as the OPC is exposed to water, but proceeds at a relatively slow pace. OPC-C must stay moist throughout the entire curing process, which may take up to 28 d.

The microstructure of hydrated OPC paste shows that two distinct types of calcium silicate hydrate form in the system: an 'inner product' and an 'outer product'. The outer product forms early during the curing process, is highly porous, and precipitates in the open spaces within the concrete structure. The inner product forms late in the curing process, is denser than the outer product, and forms near the original cement particles (Hewlett, 2006).

3.2 CSC-C curing

The low-lime CS and C_3S_2 components of CSC do not hydrate when exposed to water during the concrete mixing and forming processes. Formed CSC-C parts will not cure until they are simultaneously exposed to water and gaseous carbon dioxide. CSC-C curing is a mildly exothermic reaction in which the low-lime calcium silicates in the CSC react with carbon dioxide in the presence of water to produce calcite ($CaCO_3$) and silica (SiO_2) as shown in Reactions II and III.

II. $$CaO.SiO_2 + CO_2 \xrightarrow{H_2O} CaCO_3 + SiO_2$$

Offprint provided courtesy of www.icevirtuallibrary.com
Author copy for personal use, not for distribution

III. $3CaO.2SiO_2 + 3CO_2 \overset{H_2O}{\rightarrow} 3CaCO_3 + 2SiO_2$

The above reaction processes require an atmosphere rich in carbon dioxide. However, the process can be conducted at ambient gas pressures and at moderate temperatures (~60°C). These parameters are well within the capabilities of most precast concrete manufacturers.

Unlike the hydration reaction in OPC-C, the carbonation reaction in CSC-C is a relatively speedy process. Full curing of CSC-C is limited only by the ability of gaseous carbon dioxide to diffuse throughout the part. Thin concrete products such as roof tiles (~10 mm thick) can be cured in less than 6 h (Jain *et al.*, 2014). Larger concrete parts, such as those in railroad sleepers (~250 mm thick), can be cured within a 24 h period (Jain *et al.*, 2014). This rapid curing process can potentially enhance the productivity of existing precast operations.

Microstructural evaluation of CSC-C shows the reaction products calcite and amorphous silica as well as uncarbonated cement particles. A typical microstructure of carbon-dioxide-cured CSC-C is illustrated in Figure 1. The calcite fills the pore space within the CSC-C, creating a dense microstructure. As the silica is relatively insoluble in the prevailing conditions of the carbonation process, it forms at the outer surface of the reacting cement particle.

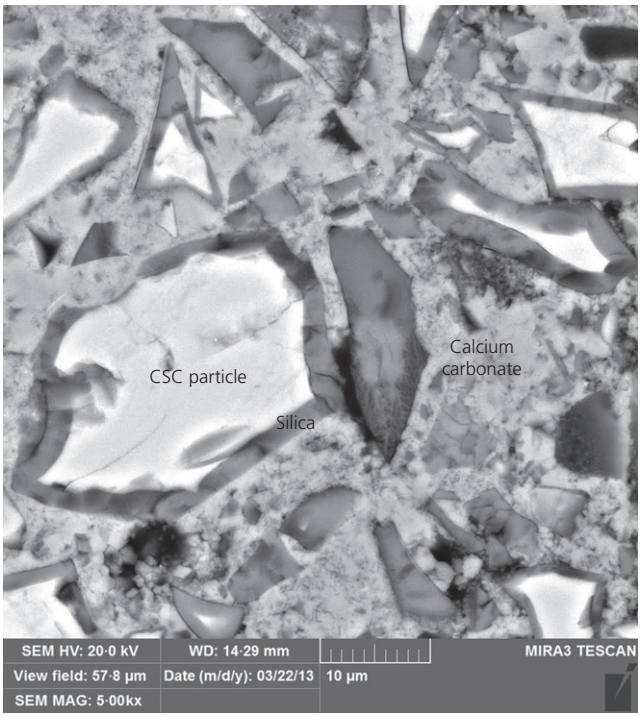

Figure 1. Microstructure of carbon-dioxide-cured CSC-C (light-grey area is calcite, dark-grey area is amorphous silica, and white area is the unreacted CSC ($CaO.SiO_2$)

3.3 Carbon dioxide utilisation in CSC-C

The unique ability of CSC-C to avoid hydration and cure using a reaction with gaseous carbon dioxide opens the possibility for the permanent sequestration of carbon dioxide in cured concrete structures. The curing processes, described in Section 3.2, enable CSC-C to utilise up to 300 kg of carbon dioxide per tonne of CSC used in the concrete formulation (DeCristofaro, 2016a). The carbon dioxide used in the curing process and captured within CSC-C is industrial-grade carbon dioxide sourced from waste flue gas streams.

Carbon dioxide utilisation in two fully cured, CSC-C forms was studied.

(*a*) Pavers of dimensions 6 cm thickness×15 cm width×23 cm length, with a dry concrete formulation of 14·7 wt% CSC, 41·6 wt% aggregate, 0·2 wt% pigment and 43·5 wt% sand (DeCristofaro, 2016a).
(*b*) A hollow core slab of dimensions 20 cm thickness×115 cm width×10 m length, with a dry concrete formulation of 15 wt% CSC, 44 wt% aggregate and 41 wt% sand (DeCristofaro, 2016b).

Small core specimens, representative of the overall concrete microstructure, were drilled from the concrete forms and exposed to the procedure described below.

To calculate the amount of carbon dioxide sequestered within a CSC-C sample, the test specimen was oven-dried at 105°C for 72 h to remove any residual moisture and placed in a furnace at 550°C for 4 h to remove any remaining bound water or organic material. Once fully dried, the specimen was heated to 950°C at a ramp-up rate of 10°C/min. After 3 h at 950°C, the specimen was reheated to 105°C and the mass loss was recorded. This mass loss was then corrected to account for mass loss from the sand and aggregate, exposed to the same procedure. The remaining mass difference represents the amount of carbon dioxide sequestered during the curing process and is attributed to the thermal decomposition of calcite, which is the primary reaction product of CSC carbonation.

The specimens taken from the CSC-C paver exhibited an average mass gain of ~3·4% due to carbon dioxide sequestration. This translates to 236 kg of carbon dioxide sequestered per tonne of CSC in the paver concrete formulation. The specimens from the CSC-C hollow core slab exhibited an average

Offprint provided courtesy of www.icevirtuallibrary.com
Author copy for personal use, not for distribution

mass gain of ~3·3%. This translated to 220 kg of carbon dioxide sequestered per tonne of CSC in the slab concrete formulation.

4. Performance and durability of CSC-based systems against OPC-based systems

4.1 Freeze–thaw resistance

Water readily enters concrete through its connected pore structure. Due to anomalous expansion during freezing, water expands by about 9%. This phenomenon exerts tensile stresses within the concrete if enough space is unavailable to accommodate the expansion. These stresses can cause the concrete to crack and, ultimately, fail (Castaneda, 2016; Powers, 1949).

To avoid failures due to repeated freezing and thawing, it is recommended that air voids are entrained into fresh concrete (PCA, 1998). These entrained air voids help to accommodate the expansion of water during freezing, thereby avoiding tensile stresses and mitigating failure in the concrete.

4.1.1 Sample preparation and testing methodology

A comparative study evaluated the performance of 76 mm × 101 mm × 405 mm OPC-C and CSC-C prisms, produced with air-entraining admixtures, under repeated freeze–thaw cycles. The mix designs used for the concrete production are shown in Table 4. The chemical composition of OPC and CSC by X-ray fluorescence (XRF) analysis is shown in Table 3. Note that equivalent amounts of cementitious material (cement, fly ash) were used for both types of concretes. In the case of CSC-C, fly ash was not used as there is no calcium hydroxide available for secondary hydration. The OPC-C prisms were demoulded after 24 h and submerged in lime-saturated water for 28 d to achieve the designed compressive strength. The CSC-C prisms were stiffer than the corresponding OPC-C prisms. Therefore, they could be demoulded immediately after forming. The CSC-C prisms were then placed on a supporting rack and inserted into the curing chamber, as shown in Figure 2. The CSC-C prisms were then cured in a 98% concentration carbon dioxide environment at 60°C for 65 h at ambient pressure (Jeong *et al*., 2014; Kuppler *et al*., 2015). More details about the curing chamber and the processes used to react specimens for this study can be found in the relevant patent (Kuppler *et al*., 2015). The carbonation reaction is an exothermic process, releasing around 87 kJ/mol of heat during curing, and the heat is dissipated through the evaporation of water contained in the concrete formulation (Atakan *et al*., 2014). The evaporated water can be condensed during circulation of the gas mixture and collected in a condenser unit (Atakan *et al*., 2014).

Table 3. Oxide composition and Blaine's fineness for OPC and CSC

	OPC	CSC
Silicon dioxide: %	19·43	44·9
Aluminium oxide: %	5·39	5·3
Ferric oxide: %	3·18	1·8
Calcium oxide: %	63·45	43·8
Magnesium oxide: %	2·97	1·2
Sulfur trioxide: %	3·38	0·3
Loss on ignition: %	0·88	NA
Sodium oxide: %	0·35	0·4
Potassium oxide: %	0·77	2·0
Free lime: %	NA	1·0
Insoluble residue: %	0·25	NA
Total alkalis as sodium oxide: %	0·86	NA
Blaine's fineness: m^2/kg	375	400

Table 4. Proportions of raw materials for concrete mixtures

	OPC-C	CSC-C
OPC: kg/m^3	325	
Calcium silicate-based cement: kg/m^3	—	400
Fly ash: kg/m^3	81	0
Sand: kg/m^3	765	689
Coarse aggregates: kg/m^3	1032	1134
Water: kg/m^3	170	116
Air-entraining admixture: ml/kg of cement	3	3
Water reducer: ml/kg of cement	0	10
Water to cementing materials	0·42	0·30

The OPC-C and CSC-C prisms were preconditioned for freeze–thaw testing by saturation in tap water for 48 h. The initial fundamental transverse frequency and mass of the saturated specimens were measured. The transverse frequency and mass were re-measured for all concrete specimens after every 30 freeze–thaw cycles.

The transverse frequency was converted into a relative dynamic modulus of elasticity (RDME) as per Equation 1.

$$1.\quad \mathrm{RDME} = \frac{(\text{Fundamental transverse frequency at } N \text{ cycles})^2}{(\text{Fundamental transverse frequency at zero cycles})^2}$$

As per ASTM C666 (ASTM, 2003), the freeze–thaw process was continued to 350 cycles or when the RDME dropped below 60%.

4.1.2 Impact on concrete performance

The RDME, calculated for both the OPC-C and CSC-C prisms after every 30 freeze–thaw cycles, is shown in Figure 3(a).

Offprint provided courtesy of www.icevirtuallibrary.com
Author copy for personal use, not for distribution

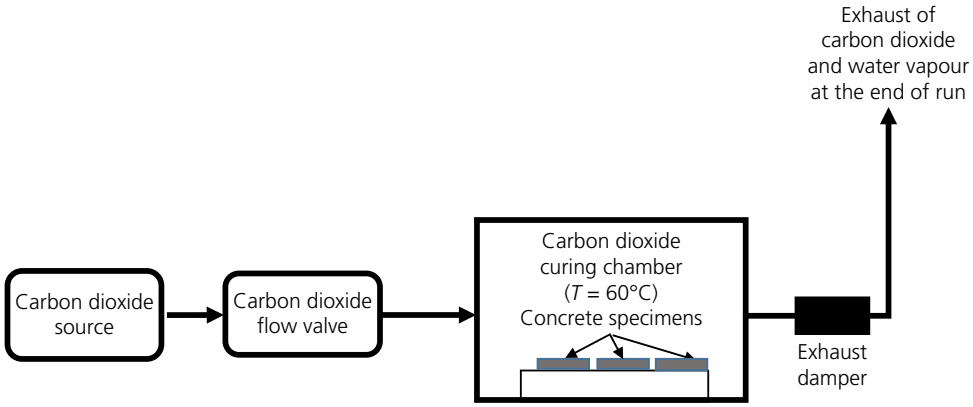

Figure 2. Curing process involved in the production of CSC concrete and mortar specimens

Both OPC-C and CSC-C prisms retained more than 90% of the RDME value after completion of 350 freeze–thaw cycles. This indicates that both OPC-C and CSC-C prisms maintained their internal structural integrity during freeze–thaw testing as per ASTM C666.

Figure 3(b) shows the normalised mass of OPC-C and CSC-C specimens. Values less than 1 indicate mass loss, while values more than 1 indicate mass gain in the concrete specimen. For the OPC-C prisms, a continuous mass loss of about 4% was observed over exposure to 350 freeze–thaw cycles. Since the RDME value for the OPC-C remained stable, the mass loss after 350 freeze–thaw cycles as per ASTM C666 can be attributed to structural damage at the surface.

In contrast, the CSC-C prisms had an initial increase in mass of about 1% during the first 100 freeze–thaw cycles. This is attributed to water absorption during the initial freeze–thaw cycles and is related to the carbon dioxide curing process described in Section 3.2. Most of the mixing water in the CSC-C prism was removed during carbon dioxide curing. Although the CSC-C prisms were soaked in water for 48 h before commencement of the test, it is presumed that the prisms were not fully saturated.

After 100 freeze–thaw cycles, no mass change was seen in the CSC-C prisms. Unlike their OPC-C counterparts, the CSC-C prisms showed no structural damage at the surface.

4.2 Scaling resistance

Scaling is local flaking or peeling of the finished surface of hardened concrete, typically as a result of repeated freezing and thawing. Scaling mechanisms may include the formation of short and discontinuous micro-cracks and loss of mortar from the surface.

4.2.1 Sample preparation and testing methodology

Concrete slabs of OPC-C and CSC-C with dimensions of 302 mm × 151 mm × 76 mm were formulated, cast and cured using the same method described in Section 4.1.1. OPC-C and CSC-C slabs were then preconditioned in air (23°C, 50% RH) for 14 d to ensure a uniform level of moisture prior to testing. A dam was installed on the top surface area of the slab to facilitate exposure to a 4% calcium chloride salt solution as specified in ASTM C672 (ASTM, 2012). The slab surfaces prior to the first freeze–thaw cycle and after 50 freeze–thaw cycles were compared.

4.2.2 Impact on concrete performance

OPC-C and CSC-C slabs from the ASTM C672 scaling tests are shown in Figures 4(a) and 4(b), respectively. Figure 4(a) shows that after 50 freeze–thaw cycles, the OPC-C slabs did not show any scaling in the form of visible aggregates or paste removal. Figure 4(b) shows that the CSC-C slab performed at a comparable level to the OPC-C slabs, with no scaling after 50 freeze–thaw cycles. This indicates that scaling resistance for both OPC-C and CSC-C is similar.

4.3 Leaching of ionic species from cement and concrete

Ionic species may leach from concrete when exposed to water. The quantity of ions entering the solution is an indirect measure of concrete durability. In the case of OPC-C, calcium hydroxide is leached into the solution, which may subsequently cause efflorescence on the surface of the concrete. Additionally, calcium hydroxide dissolution will leave behind microscopic pores in the concrete. The increased porosity allows ingress of various chemicals, such as chlorides and sulfates, into the concrete. These chemicals further deteriorate the concrete by reacting with the hydration products (Jain and Neithalath, 2009).

Offprint provided courtesy of www.icevirtuallibrary.com
Author copy for personal use, not for distribution

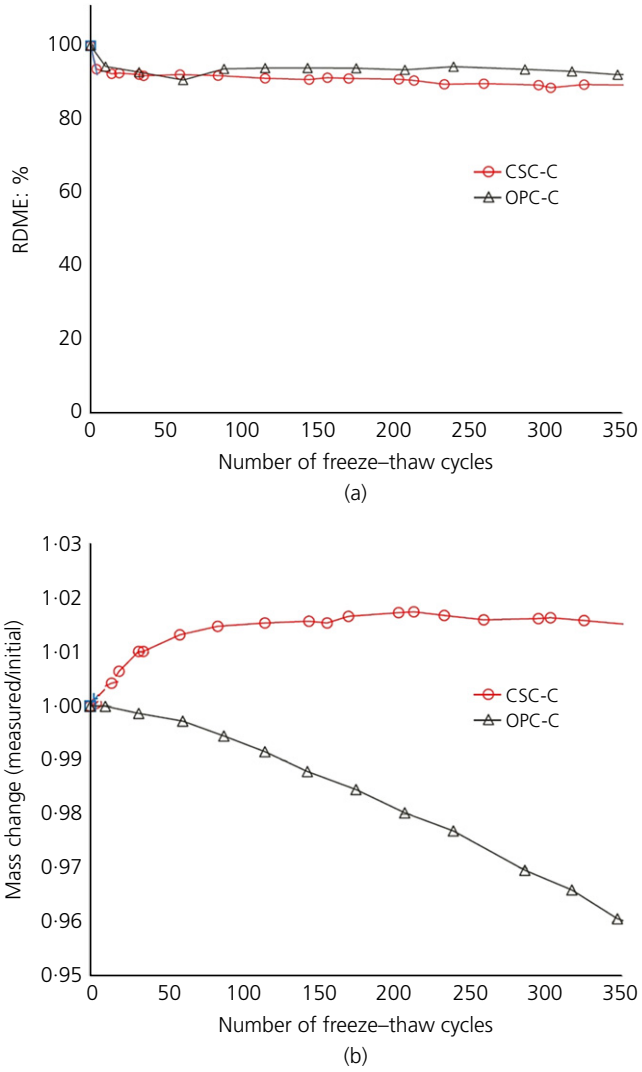

Figure 3. (a) RDME values and (b) normalised mass for CSC-C and OPC-C prisms when exposed to 350 freeze–thaw cycles

In this study, OPC-C and CSC-C specimens were exposed to deionised water for short durations. To predict the durability of these concretes in service conditions, the extent of leaching was compared.

4.3.1 Sample preparation and testing methodology

To evaluate the leaching of ionic species, 75 mm × 75 mm × 100 mm OPC-C and CSC-C specimens were formulated, cast and cured as per the procedure described in Section 4.1.1 with the following exception: the OPC-C samples were submerged in saturated lime water for 14 d. The cured specimens were then soaked in deionised water, with a solids-to-water mass ratio of 1:9. Analyses of the soak solutions after 24 h and 7 d immersions were performed using inductively coupled plasma spectroscopy (Tokpatayeva *et al.*, 2014).

4.3.2 Impact on concrete performance

The concentration of ionic species leached from CSC-C and OPC-C specimens is shown in Figure 5. After both 24 h and 7 d durations, the amount of calcium, sodium and potassium ions in the solution was much higher for the OPC-C sample than for the CSC-C sample. By contrast, less silicon leached from the OPC-C sample than from the CSC-C sample.

The calcium, sodium and potassium ions leaching from OPC-C into the solution come primarily from hydration products and unhydrated cement particles, indicating a significant loss of one or both of the reaction components. This leaching is detrimental to the integrity of the concrete matrix.

For CSC-C, the calcium, sodium and potassium ions are bonded in the form of insoluble carbonates. Hence, relatively few ions enter the soak solution and the impact on concrete strength is expected to be minimal. The low level of alkali ion dissolution from CSC-C is also expected to improve the resistance to alkali–silica reaction.

4.4 Efflorescence from concrete pavers

Efflorescence is the formation of white crystalline salts, such as calcium carbonates, on the surface of concrete. This phenomenon is considered to be an aesthetic defect in architectural concrete products. Efflorescence is caused by the diffusion of water-soluble species, such as calcium hydroxide, from the interior of the cured concrete to the surface, where it reacts with atmospheric carbon dioxide to create the white carbonate. The carbonation reaction is accompanied by a mass gain. The tendency of efflorescence in OPC-C and CSC-C can thus be compared using mass gain measurements after prescribed and controlled exposures.

4.4.1 Sample preparation and testing methodology

OPC-C and CSC-C pavers were formed utilising a commercial mix design with charcoal pigment to highlight the white deposits more clearly. The mix design used for the production of these pavers consisted of 275 kg/m^3 of cement (OPC or CSC), 883 kg/m^3 of sand, 645 kg/m^3 of 6·75 mm aggregates, 157 kg/m^3 of recycled concrete aggregates (9·5 mm) and 0·55 kg/m^3 of pigment. The water-to-cement ratio was 0·32 for both paver types. OPC-C pavers were air-dried for 3 d after production. Correspondingly, CSC-C pavers were carbon-dioxide-cured for 36 h in a chamber at ambient pressure as per the procedure described in Section 4.1.1.

The method used for evaluating the efflorescence in OPC-C and CSC-C pavers involved partially submerging paver

Offprint provided courtesy of www.icevirtuallibrary.com
Author copy for personal use, not for distribution

Figure 4. OPC-C (a) and CSC-C (b) specimens before and after completion of 50 freeze–thaw cycles in scaling tests

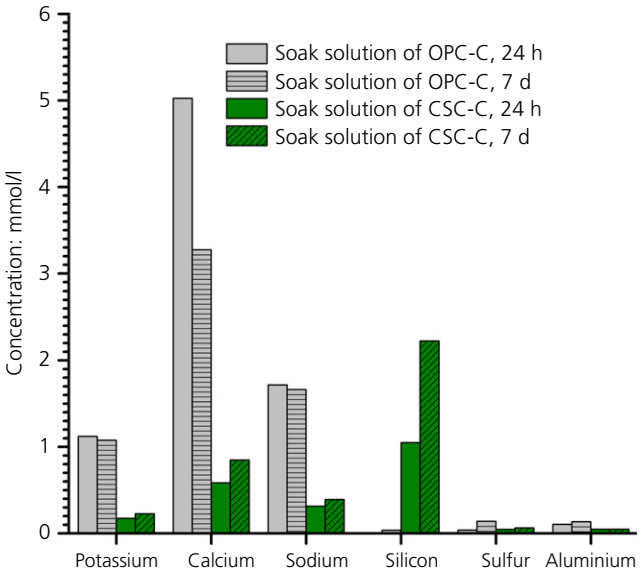

Figure 5. Leaching of ionic species from CSC-C or OPC-C after soaking in deionised water for 24 h and 7 d

samples in deionised water (Ashraf *et al.*, 2014; Nhar *et al.*, 2007). The apparatus for testing 100 mm × 60 mm × 15 mm paver samples is shown in Figure 6. The mass change in each sample was recorded after 14, 28 and 91 d of submersion in deionised water in an environment of 23°C and 50% RH.

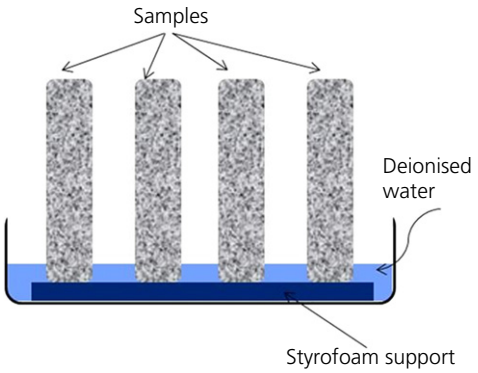

Figure 6. Efflorescence test set-up

The samples were periodically removed from the set-up and dried in a 100°C oven for 24 h. The mass of the dried sample was recorded and the mass of efflorescence was then expressed as relative mass change w_{To} according to the formula

$$2. \quad w_{To} = \frac{w_2 - w_1}{w_1} \times 100$$

where w_{To} is the relative mass change (%), w_1 is the weight of the dried sample prior to submersion in water (g) and w_2 is the weight of the dried sample after completion of submersion in water (g).

Offprint provided courtesy of www.icevirtuallibrary.com
Author copy for personal use, not for distribution

4.4.2 Impact on concrete performance

Figure 7 shows the relative mass change of the OPC-C and CSC-C pavers after different submersion durations. The OPC-C pavers showed larger mass gain, and therefore greater degrees of efflorescence, after all submersion durations when compared with the CSC-C pavers. The presence of calcium hydroxide, as a reaction product in OPC-C curing, facilitates the mass gain through leaching and subsequent carbonation. In contrast, in CSC-C the calcium is primarily present as insoluble calcium carbonate due to carbonation curing. This is in line with the observations from the results mentioned in Section 4.3, which showed greater dissolution of calcium ions in the soak solution of OPC-C.

Thus, it can be concluded that CSC-C products are less susceptible to calcium carbonate efflorescence than OPC-C products. The reduced susceptibility to calcium carbonate efflorescence makes CSC-C product a very lucrative option for architectural concrete applications by eliminating the expensive remedial measures that can be necessary in OPC-C products.

4.5 Expansion in mortar bars when exposed to sulfate solution

One of the sources of sulfate attack is penetration of soluble sulfates from surrounding groundwater into concrete. During this type of sulfate attack, ettringite ($Ca_6Al_2(OH)_{12}(SO_4)_3.26H_2O$) is formed from the monosulfate hydrate ($Ca_4Al_2(OH)_{12}(SO_4).6H_2O$) that is present in OPC-C.

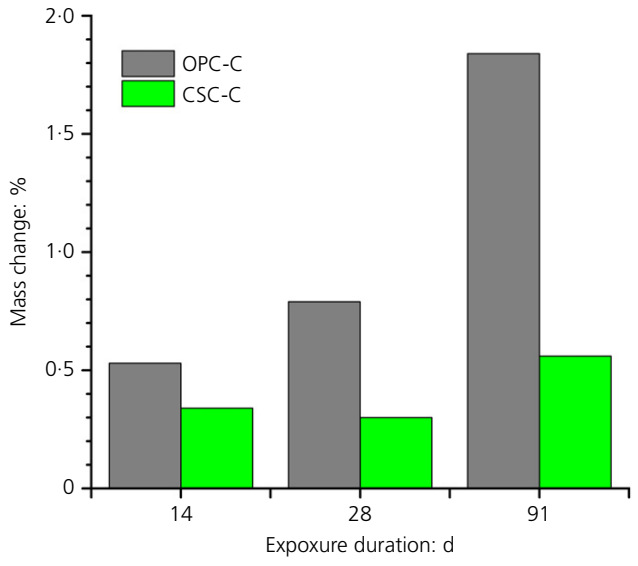

Figure 7. Comparison of mass change for CSC-C and OPC-C pavers against exposure duration

This leads to the precipitation of ettringite during sulfate attack.

IV. $$Ca_4Al_2(OH)_{12}(SO_4).6H_2O \rightarrow 4Ca^{2+} + 2Al(OH)_4{}^- + 4(OH)^- + SO_4{}^{2-} + 6H_2O$$

V. $$6Ca^{2+} + 2Al(OH)_4{}^- + 4(OH)^- + 3SO_4{}^{2-} + 26H_2O \rightarrow Ca_6Al_2(OH)_{12}(SO_4)_3.26H_2O$$

Ettringite formation is associated with local volume expansion in the brittle concrete matrix. This undermines the bond between cement paste and aggregate within the concrete.

Reactions IV and V indicate that a source of ionic calcium (Ca^{2+}) is necessary for the growth of ettringite. Calcium hydroxide acts as this source, as shown in Reaction VI, and is the first crystal from the cement paste to dissolve according to the following reaction.

VI. $$Ca(OH)_2 \rightarrow Ca^{2+} + 2OH^-$$

Although the above effects are typical of attack by solutions of sodium sulfate, solutions containing magnesium sulfate can be more aggressive. Therefore, in this study, OPC-based mortar (OPC-M) and CSC-based mortar (CSC-M) specimens were exposed to both sodium sulfate and magnesium sulfate solutions. Based on leaching experiments, it was expected that the CSC-M specimens would perform well since the calcium, sodium and potassium ions are locked in as carbonates in the CSC-C and thus less concentrations of these ions are leached as compared with OPC-C samples.

4.5.1 Sample preparation and testing methodology

The OPC-M samples were prepared according to ASTM C109-12 (ASTM, 2013a). After demoulding, the OPC-M specimens were cured in saturated lime water at 23°C for 28 d. The CSC-M bars were prepared with modified ASTM C109 using CSC and ASTM C77 graded standard sand (Ottawa sand) where water-to-cement ratio of 0·30 was used. Immediately after casting, the CSC-M bars were carbonated for 24 h at 65°C in the environmental chamber as mentioned in Section 4.1.1. As per ASTM C1012, the resulting 25 mm × 25 mm × 285 mm mortar bars were immersed in 0·35 M solutions of sodium sulfate and magnesium sulfate with a solid-to-solution volume ratio of 1:4 (ASTM, 2013b; Tokpatayeva *et al.*, 2016). Measurements of length and mass changes were performed at prescribed time intervals.

Offprint provided courtesy of www.icevirtuallibrary.com
Author copy for personal use, not for distribution

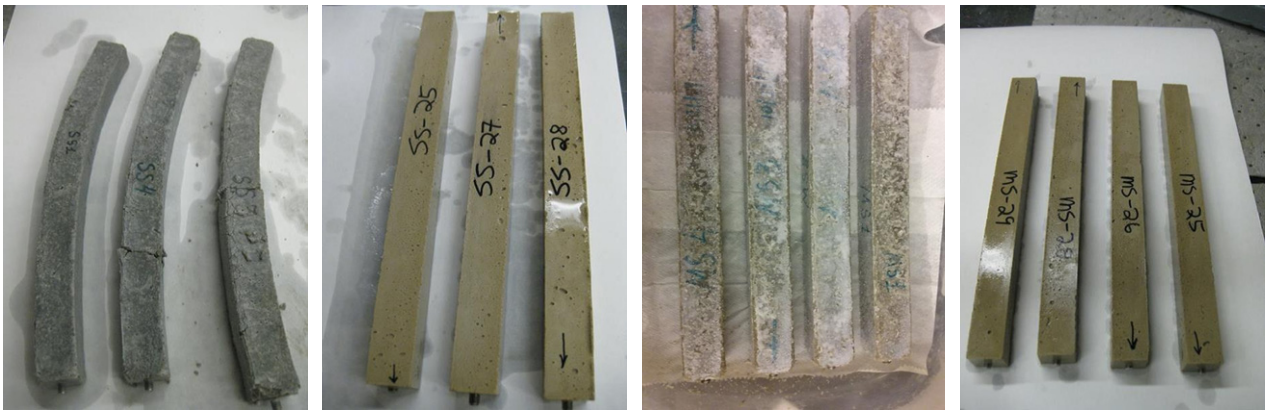

(a) (b) (c) (d)

Figure 8. Mortar bar specimens exposed to sodium sulfate (a) and (b), and magnesium sulfate (c) and (d): (a) and (c) OPC-M after ~9 months of exposure; (b) and (d) CSC-M after 18 months of exposure

4.5.2 Impact on concrete performance

Figures 8(a) to 8(d) illustrate the appearance of the OPC-M (Figures 8(a) and 8(c)) and CSC-M (Figures 8(b) and 8(d)) bars after 9 and 18 months of exposure, respectively, to sodium sulfate (Figures 8(a) and 8(b)) and magnesium sulfate (Figures 8(c) and 8(d)) solutions. OPC-M bars exposed to either sulfate solutions showed severe shape changes or cracking. In contrast, the shape and appearance of the CSC-M bars remained unchanged during the entire exposure period.

The shape changes of OPC-M and CSC-M shown in Figure 8 are converted to length change measurements in Figure 9. The length change in the OPC-M bars in both sulfate solutions exceeded the ASTM C1012 threshold of 0·10% in 30 weeks or less. In contrast, the length change in the CSC-M bars was seen to be below 0·05%, even after 72 weeks of exposure in both solutions. The performance of the CSC-M bars exceeded the reported performance observed in mortar bars prepared with type V sulfate-resistant OPC (Irassar *et al.*, 2000).

Figure 10 shows the mass change due to sulfate uptake in OPC-M bars and CSC-M bars exposed to sodium sulfate and magnesium sulfate solutions. The OPC-M bars exhibited a continuous mass gain up to the point of failure. In contrast, the CSC-M bars showed a mass gain only up to 15 weeks and thereafter stabilised. Moreover, no failure was seen in the CSC-M bars, even after 50 weeks of exposure.

The instability of the OPC-M bars seen in the above results is directly attributed to the ettringite formation stimulated by high ionic calcium concentrations, as described in Section 4.3.2. The absence of ionic calcium in the CSC-M bars suppressed the formation of ettringite, facilitating dimensional stability. Thus, concrete systems based on CSC will be more resistant to sulfate attack.

5. Conclusions

5.1 Environmental considerations

(*a*) The unique, low-lime content of the CSC clinker enables two separate opportunities to reduce carbon dioxide emissions at cement plants. The carbon dioxide released from the chemical decomposition of limestone will be reduced from 540 kg/t of OPC clinker to about 375 kg of carbon dioxide per tonne of CSC clinker. Additionally, the low-lime chemistry of CSC allows the reaction between lime and silica to occur at temperatures 250°C lower than that required for OPC clinker formation, reducing the carbon dioxide emissions associated with the burning of fossil fuel from 270 to 190 kg/t. This makes it possible to reduce the carbon dioxide emissions from ~810 kg/t of OPC clinker to ~565 kg/t of CSC clinker.

(*b*) The unique ability of CSC to avoid hydration and cure using a reaction with gaseous carbon dioxide opens up the possibility of the permanent sequestration of carbon dioxide in cured concrete structures. The curing processes enable CSC-C to sequester up to 300 kg of carbon dioxide per tonne of CSC used in the concrete formulation. The carbon dioxide used in the curing process and captured within CSC-C is industrial-grade carbon dioxide sourced from waste flue gas streams.

(*c*) Depending on the specific ratios of sand, aggregate and CSC used in the concrete mix, the final CSC-C part may contain between about 3 and 7 wt% of sequestered carbon dioxide.

Offprint provided courtesy of www.icevirtuallibrary.com
Author copy for personal use, not for distribution

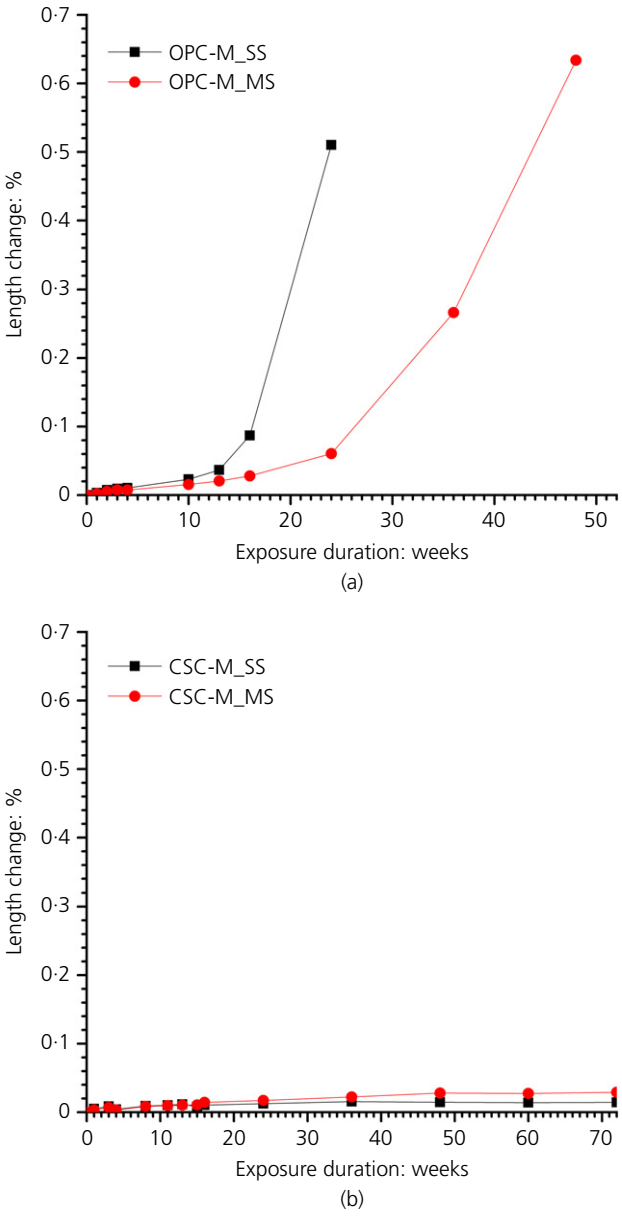

Figure 9. Length changes in (a) OPC-M after ~9 months of exposure and (b) CSC-M after 18 months of exposure to sodium sulfate (SS) and magnesium sulfate (MS) solutions

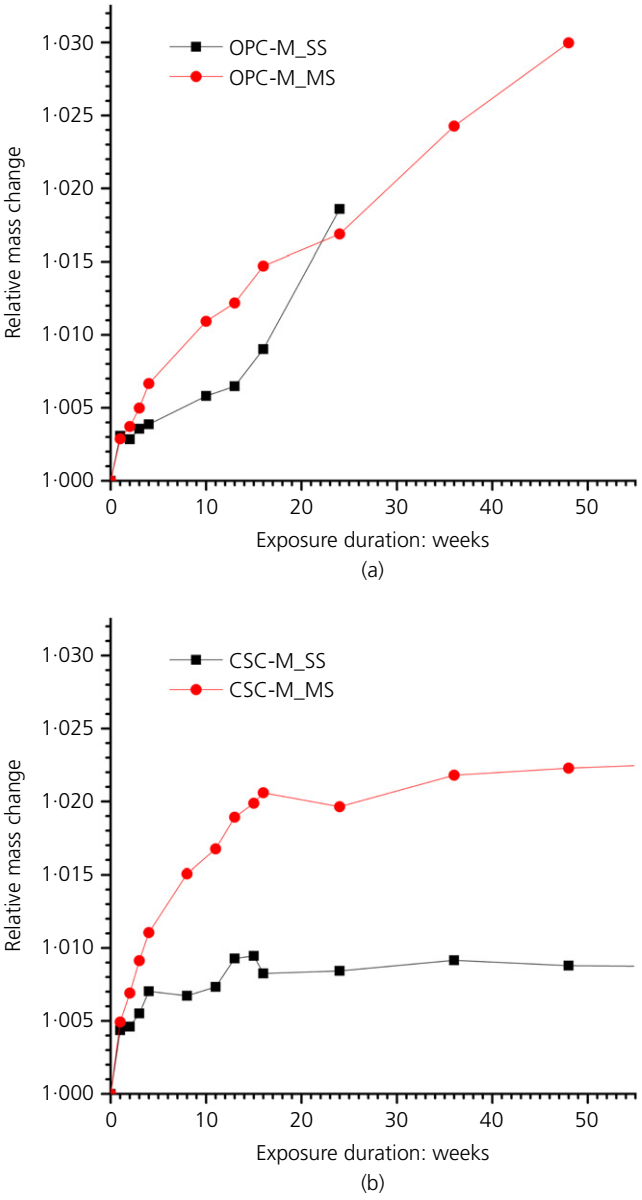

Figure 10. Relative mass changes in (a) OPC-M after ~9 months of exposure and (b) CSC-M after 18 months of exposure to sodium sulfate (SS) and magnesium sulfate (MS) solutions

(*d*) The combined effects of (*a*), (*b*) and (*c*) offer the potential to reduce the carbon dioxide footprint associated with the production and use of 1 t of cement from 810 kg of carbon dioxide for OPC to 265 kg for CSC.

(*e*) Unlike OPC-C, concrete products hardened with carbon-dioxide-cured CSC do not consume water. Thus, if necessary, all the water used in the CSC-C formulation can be recovered during the carbon dioxide curing process.

5.2 Durability considerations

(*a*) CSC-C prisms performed similar to or better than OPC-C prisms in terms of freeze–thaw resistance and scaling resistance. This allows CSC-C and OPC-C to be used interchangeably.

Offprint provided courtesy of www.icevirtuallibrary.com
Author copy for personal use, not for distribution

(*b*) The amounts of ionic calcium, potassium and sodium leached into solution from OPC-C exceeded the amounts from CSC-C. The significant reduction of these ionic species in CSC-C improves the chemical stability of this concrete system. Thus, a superior performance is expected from CSC-C in applications where concrete is exposed to water.

(*c*) CSC-C products are less susceptible to calcium carbonate efflorescence than OPC-C products. The reduced susceptibility to calcium carbonate efflorescence makes CSC-C product a very lucrative option for architectural concrete applications by eliminating expensive remedial measures necessary in OPC-C products.

(*d*) The absence of ionic calcium in CSC-C products suppresses the formation of ettringite when concrete is attacked by sulfate salts, which facilitates dimensional stability. In the face of sulfate attack, concrete systems based on CSC will exhibit dimensional stability superior to that of OPC-C or concrete based on sulfate-resistant cements.

Acknowledgements

The authors acknowledge Lyles School of Civil Engineering, Purdue University, West Lafayette, Indiana, USA, for performing all tests described in this paper under a research programme sponsored by Solidia Technologies Inc.

REFERENCES

Ashraf W, Jeong H, Olek J and Jain J (2014) An experimental investigation of the selected properties of calcium silicate based carbonated concrete (CSCC) systems. *Presented at ACI Fall Convention, Washington, DC, USA*.

ASTM (2003) C666: standard test method for resistance of concrete to rapid freezing and thawing. ASTM International, West Conshohocken, PA, USA.

ASTM (2012) C672: standard method for scaling resistance of concrete surfaces exposed to deicing chemicals. ASTM, West Conshohocken, PA, USA.

ASTM (2013a) C109: standard method for compressive strength of hydraulic cement mortars (using 2-in. [50 mm] cube specimens). ASTM International, West Conshohocken, PA, USA.

ASTM (2013b) C1012: standard test method for length change of hydraulic-cement mortars exposed to a sulfate solution. ASTM International, West Conshohocken, PA, USA.

Atakan V, Sahu S, Quinn S, Hu X and DeCristofaro N (2014) Why CO_2 matters – advances in a new class of cement. *ZKG International* (**3**).

Barcelo L, Kline J, Walenta G and Gartner E (2014) Cement and carbon emission. *Materials and Structures* **47(6)**: 1055–1065.

Boden TA, Marland G and Andres RJ (2014) *Global, Regional, and National Fossil-Fuel CO_2 Emissions.* Carbon Dioxide Information Analysis Center, Oak Ridge, TN, USA.

Castaneda D (2016) *Freeze–Thaw Environment of Precast Concrete Crossties and Effect of Vibration on Fresh Materials.* PhD dissertation, University of Illinois at Urbana, Champaign, IL, USA.

DeCristofaro N (2016a) *Utilization of CO_2 in High Performance Building and Infrastructure Products.* A report on work under agreement DE-FE0004222 for U.S. Department of Energy, National Energy Technology Laboratory, Piscataway, NJ, USA. See https://www.osti.gov/scitech/servlets/purl/1301860 (accessed 03/10/2017).

DeCristofaro N (2016b) *Solidia Concrete – A Sustainable Method for Cement Production and CO_2 Utilization*. K130123 Final Report to Climate Change and Emissions Management Corporation Grand Challenge Innovative Carbon Usage, Piscataway, NJ, USA.

DeCristofaro N and Sahu S (2013) *Solidia Cement™ Part One of a Two-Part Series Exploring the Chemical Properties and Performance Results of Sustainable Solidia Cement™ and Solidia Concrete™*. Solidia Technologies, Piscataway, NJ, USA. See http://solidiatech.com/wp-content/uploads/2014/02/Solidia-Cement-White-Paper-12-17-13-FINAL.pdf (accessed 03/10/2017).

DeCristofaro N, Meyer V, Sahu S, Bryant J and Moro F (2017) Environmental impact of carbonated calcium silicate cement-based concrete. *Proceedings of 1st International Conference on Construction Materials for Sustainable Future, CoMS, Zadar, Croatia*.

EPA (Environmental Protection Agency) (2005) *AP42 – Compilation of Air Pollutant Emission Factors, Vol. 1; Stationary Point and Area Sources.* EPA, Washington, DC, USA.

Hewlett PC (2006) *Lea's Chemistry of Cement and Concrete.* Elsevier, Oxford, UK.

IPCC (Intergovernmental Panel on Climate Change) (2007) *Climate Change 2007: Mitigation*. Contribution of Working Group III to the Fourth Assessment Report. Intergovernmental Panel on Climate Change. Section 7.4.5.1: Minerals – Cement.

Irassar E, Gonzalez M and Rahhal V (2000) Sulfate resistance of type V cements with limestone filler and natural pozzolana. *Cement & Concrete Composites* **22(5)**: 361–368.

Jain J and Neithalath N (2009) Analysis of calcium ion leaching behavior of plain and modified cement pastes in pure water. *Cement & Concrete Composites* **31(3)**: 176–185.

Jain J, Deo O, Sahu S and DeCristofaro N (2014) *Solidia Concrete™ Part Two of a Series Exploring the Chemical Properties and Performance Results of Sustainable Solidia Cement™ and Solidia Concrete™*. Solidia Technologies, Piscataway, NJ, USA. See http://solidiatech.com/wp-content/uploads/2014/02/Solidia-Concrete-White-Paper-FINAL-2-19-14.pdf (accessed 03/10/2017).

Jeong H, Olek J, Jain J, Ravikumar D and Atakan V (2014) Freeze–thaw and scaling resistance of calcium silicate based carbonated concretes. *Presented at ACI Fall Convention, Washington, DC, USA*.

Kuppler JP, Atakan V, Smith K and Hu X (2015) *Curing Systems for Materials that Consume Carbon Dioxide and Method Thereof.* US Patent 9 221 027 B2, Dec.

Madlool NA, Saidur R, Hossain MS and Rahim NA (2011) A critical review on energy use and savings in the cement industries. *Renewable and Sustainable Energy Reviews* **15(4)**: 2042–2060.

Marceau ML, Nisbet MA and VanGeem MG (2006) *Life Cycle Inventory of Portland Cement Manufacture, SN2095b.* Portland Cement Association, Skokie, IL, USA.

Nhar H, Watanabe T, Hashimoto C and Nagao S (2007) *Efflorescence of Concrete Products for Interlocking Block Pavements.* American Concrete Institute, Farmington Hills, MI, USA, SP 243-2, pp. 19–34.

PCA (Portland Cement Association) (1998) Control of air content in concrete. *Concrete Technology Today* **19(1)**: 1–8.

Powers TC (1949) The air requirement of frost-resistant concrete. *Proceedings of the Highway Research Board, PCA Bulletin 33*,

Offprint provided courtesy of www.icevirtuallibrary.com
Author copy for personal use, not for distribution

Portland Cement Association, Skokie, IL, USA, vol. 29, pp. 184–211.

Riman RE and Atakan V (2012) Systems and methods for carbon capture and sequestration and compositions derived therefrom. US Patent 8 114 367, Feb.

Riman RE, Gupta S, Atakan V and Li Q (2013) *Bonding Element, Bonding Matrix and Composite Material Having The Bonding Element, and Method of Manufacturing Thereof*. US Patent Application 0122267, May.

Taylor HFW (1997) *Cement Chemistry*, 2nd edn. Thomas Telford, London, UK.

Tokpatayeva R, Olek J, Jain J, Ravikumar D and Atakan V (2014) Solidia cement – A novel calcium silicate-based cement-microstructure and soak-solution chemistry, Poster presentation. In *5th Advances in Cement-Based Materials: Characterization, Processing, Modeling and Sensing*, Tennessee Technological University, Cookeville, TN, USA.

Tokpatayeva R, Olek J, Sahu S and Jain J (2016) Comparative study of sulfate attack resistance of carbonated calcium silicates and plain Portland cement mortars. In *7th Advances in Cement-Based Materials (Cements 2016)*, Northwestern University, Evanston, IL, USA.

UNEP (United Nations Environment Programme) (2010) *Greening Cement Production*. United Nations Environment Programme, Sioux Falls, SD, USA.

WBCSD (World Business Council for Sustainable Development) (2009) *Cement Technology Roadmap 2009: Carbon Emissions Reductions Up to 2050*. World Business Council for Sustainable Development, Geneva, Switzerland.

How can you contribute?

To discuss this paper, please email up to 500 words to the editor at journals@ice.org.uk. Your contribution will be forwarded to the author(s) for a reply and, if considered appropriate by the editorial board, it will be published as discussion in a future issue of the journal.

Proceedings journals rely entirely on contributions from the civil engineering profession (and allied disciplines). Information about how to submit your paper online is available at www.icevirtuallibrary.com/page/authors, where you will also find detailed author guidelines.